Enhanced removal of selenate from mining effluent by H_2O_2/HCl-pretreated zero-valent iron

Bing Wu, Huichao Jia, Zhe Yang, Chao Shan, Jingxia Weng, Zhe Xu and Bingcai Pan

ABSTRACT

Direct use of zero-valent iron (ZVI) in reductive removal of selenate (Se(VI)) is inefficient due to the intrinsic passive layer of ZVI. Here we observed that ZVI pretreated with H_2O_2 (P-ZVI-O) performs much better in Se(VI) removal from a mining effluent than other three modes of ZVI alone, acid washing ZVI (P-ZVI-A), and simultaneous addition of H_2O_2 and ZVI (ZVI-O) as well. The P-ZVI-O exhibits exceptionally high Se(VI) removal at a low dosage, wide pH range, with Se dropping down from 93.5 mg/L to <0.4 μg/L after 7-h reaction. Interestingly, the initial pH (2–6) of the mining effluent exerted little influence on the final Se(VI) removal. H_2O_2/HCl pretreatment results in the formation of various reducing corrosion products (e.g. Fe_3O_4, FeO and Fe^{2+}), which greatly favors the efficient Se(VI) removal. In addition, surface-bound Fe^{2+} ions participated in the reduction of Se (VI). Combined with the influence of Se valence as well as pH and Fe^{2+} (whether dissolved or surface bound), it is deduced that the P-ZVI-O mode induced efficient Se(VI) removal via the adsorption-reduction and/or co-precipitation. This study demonstrates that H_2O_2/HCl pretreatment of ZVI is a very promising option to enhance the efficiency of reductive removal of Se(VI) from real effluents.

Key words | H_2O_2, mining effluent, pretreatment, selenate, zero-valent iron

Bing Wu†
Huichao Jia†
Zhe Yang
Chao Shan
Jingxia Weng
Zhe Xu
Bingcai Pan (corresponding author)
State Key Laboratory of Pollution Control and Resource Reuse, School of the Environment,
Nanjing University,
Nanjing 210023,
China
E-mail: *bcpan@nju.edu.cn*

†Both contributed equally to this work.

INTRODUCTION

Selenium (Se) is an essential trace element to human. However, excessive exposure of Se could cause various adverse effects, such as skin rash and nerve damage. Se in natural water mainly originates from human activities such as mining, agriculture and industrial operations (Xie *et al.* 2015). In general, inorganic Se mainly exists in four valences, including selenide (Se(-II)), elemental Se (Se(0)), selenite (Se(IV)) and selenate (Se(VI)). Among them, Se(IV)) and Se(VI) received most attention in water treatment because of their high bioavailability and potential toxicity (Winkel *et al.* 2012). Nowadays, the maximum limited concentration of total Se in drinking water and wastewater discharge is 0.01 mg/L and 0.1 mg/L, as regulated by China, respectively.

Generally, Se(IV) in water can be readily and specifically adsorbed by various kinds of metal oxides, such as Fe(III) and Mn(IV) oxides, through the formation of inner-sphere complexes (Xie *et al.* 2015). As for Se(VI) removal, several processes, including adsorption, ion exchange, membrane technology, and coagulation were tested; nevertheless, most of them are far from satisfactory (Kang *et al.* 2004; Fu & Wang 2011). Compared with the above processes, biological treatment has the potential not only to remove selenium from water, but also to sequester it in a reusable form (Nancharaiah & Lens 2015). Despite these advantages, the bio-process may not work for certain industrial and mining effluents due to the extreme conditions unsuitable for microorganism's growth, such as acidic pH, high salinity and xenobiotic compounds. Therefore, reduction of Se(VI) to Se(IV) or other low-valence state and then removal via adsorption or other separation processes is regarded as a promising option for Se(VI) removal from actual effluents (Kang *et al.* 2015). Among the reduction processes, zero-valent iron (ZVI) technology

doi: 10.2166/wst.2018.526

exhibits great potential for Se(VI) removal via reduction and adsorption (Ling *et al.* 2015) in consideration of its cost effectiveness, availability and environmental friendliness (Guan *et al.* 2015).

As is well known, the pristine ZVI is usually covered with an intrinsic passive layer due to the air-induced slow oxidation, which inevitably reduces its reactivity significantly (Liang *et al.* 2014). To activate ZVI, it is necessary to remove the passive layer and expose the inner active substance of ZVI (Guan *et al.* 2015). Pretreatment of ZVI with H_2, acidic washing, ultrasonication and premagnetization were the common countermeasures for this issue. H_2 or acidic washing pretreatment could destroy the passive layer to expose the fresh iron; however, the fresh surface would be quickly re-passivated in aqueous solution by H_2O/O_2 (Guan *et al.* 2015). As for the ultrasonication and premagnetization, its application in practice would be a great challenge in consideration of the large treatment unit, which would significantly increase the cost and complexity.

Recently, a combination of ZVI/oxidants system was found to accelerate the corrosion of ZVI and greatly improve the removal of toxic metals or inorganic ions, such as arsenic, selenate, mercury, cadmium and nitrate (Katsoyiannis *et al.* 2015; Guo *et al.* 2016; Yang *et al.* 2016). The strong oxidants significantly enhanced corrosion of ZVI, resulting in the generation of iron (hydr)oxides capable of removing contaminants via adsorption, precipitation, coprecipitation, size-exclusion and possible reduction (Tang *et al.* 2016). In particular, the formation of iron oxides (Fe_3O_4/FeO) are available for reduction/removal of Se(VI) (Segura *et al.* 2015). Based on the above enlightenment, our group found that pretreating ZVI with H_2O_2/HCl can significantly enhance reductive performance of ZVI/H_2O system for nitrate and nitrobenzene (Yang *et al.* 2018a, 2018b). However, the feasibility of the H_2O_2/HCl pretreatment system (termed as P-ZVI-O) in performing the reductive transformation of Se(VI) in the mining effluent is still unclear.

The main objective of this study is to explore the performance of different ZVI modes, i.e. P-ZVI-O, acid pretreated ZVI (P-ZVI-A), simultaneous addition of H_2O_2 and ZVI (ZVI-O), as well as its direct use, in the efficiency of ZVI system for Se(VI) removal from a real smelting wastewater. Afterwards, the evolution of solution chemistry including pH, Fe^{2+} (dissolved or surface bound), and the oxidation/reduction potentials, during the process of the optimized mode were also investigated to preliminarily probe the underlying mechanism for Se(VI) removal.

MATERIALS AND METHODS

Materials

All chemicals used in this study were of analytical reagent grade. ZVI of 80–100 mesh was purchased from Sinopharm Chemical Shanghai Reagent Co., Ltd (China). H_2O_2 (30%) was purchased from Nanjing Chemical Reagent Co., Ltd. The mining effluent containing selenate was sampled from a smelting plant in Huangshi, Hubei Province, China.

Pretreatment of ZVI

Pretreatment of ZVI with H_2O_2/HCl (i.e. P-ZVI-O) was conducted as follows: firstly, 25 mL water was added into a 150-mL conical flask and the pH value was adjusted to 1.5 with 50% HCl. ZVI and H_2O_2 at preset levels were added into the flask. Then, the mixtures were sealed and transferred to a shaker immediately. After shaking for 1 h, the suspension was used for subsequent Se removal. Note that the initial pH of the suspension and the wastewater were adjusted to the same values for subsequent removal experiments. Pretreatment of ZVI with acid (i.e. P-ZVI-A) was conducted by the similar procedure as P-ZVI-O. Pristine ZVI without any pretreatment was also employed as control. In addition, pristine ZVI and H_2O_2 (i.e. ZVI-O) were simultaneously added into the target wastewater to compare and identify the role of H_2O_2 in the process of Se(VI) removal.

Batch experiments

For batch experiments, the P-ZVI-O suspension (25 mL) was adjusted to pH 3.22 and added into 25 mL wastewater directly, and the initial pH was kept constant during mixing. To keep uniform, the ZVI and ZVI-O groups were conducted using diluted water samples (25 mL wastewater sample + 25 mL pure water) and at the same pH value as the above mode. For the ZVI-O group, after mixing ZVI with the target wastewater, H_2O_2 was immediately added. All samples were sealed to inhibit the reaction between dissolved oxygen and reductive species. All the experiments were conducted in the shaker.

Analytical methods

Dissolved Se(VI) and Se(IV) was determined by the atomic fluorescence spectrometry (AFS, AF-640A, Beifen-Ruili)

with a detection limit of 0.4 μg/L. Samples were firstly treated by 10% $HClO_4$-HNO_3 (1:1) for degradation and then 5 mL 50% HCl for reduction. The samples were adjusted to 20% HCl content for detection. Concentration of dissolved Fe ions was measured based on the 1,10-phenanthroline spectrophotometric method at the absorbance wavelength of 510 nm. Concentration of the surfaced-associated Fe^{2+} was measured by addition of phenanthroline prior to filtration. The H_2O_2 content was measured by the titanium oxalate method. Zeta potential of the solution was determined by Malvern Zetasizer Nano ZS90 (Malvern, UK).

Characteristics of iron and selenium substance

Solid phase produced from different modes was applied for characteristics of Fe and Se substance. All the samples were frozen by liquid nitrogen and dried using a freeze-drying reactor. The samples were stored under vacuum prior to further analysis. X-ray diffraction (XRD) was used to determine the crystalline of ferric substance by X-TRA (ARL, Switzerland). The surface morphology was measured by the scanning electron microscope (SEM-EDX, S-3400N II, Hitachi, Japan). X-ray photoelectron spectroscopy (XPS) was used to analyze the Se valence based on PHI 5000 VersaProbe (UIVAC-PHI, Japan).

RESULTS AND DISCUSSION

Se(VI) removal of different ZVI usage modes

Some basic properties of the wastewater sample are shown in Table 1. Four ZVI utilization modes, including ZVI, ZVI-O, P-ZVI-A, and P-ZVI-O, were applied in the actual wastewater treatment for comparison. Figure 1 shows the Se(VI) removal of four modes within 25-h reaction. Slight improvement in Se(VI) removal by P-ZVI-A over ZVI indicated that acidic washing was not a satisfactory choice. For ZVI-O with the addition of H_2O_2, H_2O_2 significantly improved the Se(VI) removal efficiency by ZVI, and more than 87% of Se(VI) was removed after 25 h.

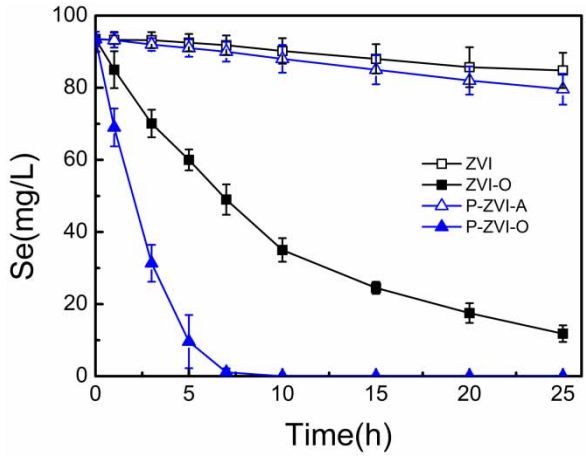

Figure 1 | Removal of Se(VI) by four ZVI utilization modes. The initial pH was 3.2 ± 0.1, and dosages of ZVI and H_2O_2 were 10 g/L and 0.4 M, respectively.

Attractively, P-ZVI-O could result in a complete removal of Se(VI) in 7 h, performing much better than the previous reports (Yoon *et al.* 2011; Tang *et al.* 2014). For example, 10 g/L ZVI combined with 10 g/L Fe_3O_4 and 0.5 mM Fe^{2+} could effectively remove Se(VI) at the initial concentration of 20 mg/L, and 33 g/L ZVI and 26-h reaction time were required to remove 50% Se(VI) at 300 mg/L initially. Obviously, P-ZVI-O is very promising to remove Se(VI) from industrial wastewater. In the following experiments, only the mode of P-ZVI-O was considered.

Optimization of the operational conditions

Removal of Se(VI) by P-ZVI-O was examined as a function of H_2O_2 concentration, ZVI dosage, and pHs. As shown in Figure 2(a), Se(VI) removal was completely achieved for 0.4 M H_2O_2 at pH 1.5 within 7 h. Further increase in H_2O_2 concentration accompanied with a negative effect on Se(VI) removal, which was probably due to the consumption of reductive species by excessive H_2O_2 (Yoon *et al.* 2016). In the following experiments, we set the concentration of H_2O_2 at 0.40 M.

Effect of ZVI dosage was also studied at the H_2O_2 dosage of 0.40 M (Figure 2(b)). Removal of Se(VI) was significantly enhanced with the increase of ZVI concentration.

Table 1 | Basic compositions of the target wastewater used in this study (mg/L)[a]

Na^+	K^+	SO_4^{2-}	Cl^-	Si	Se(VI)	Fe	Ca
17389 ± 842.5	29 ± 3.6	6350 ± 566.1	19100 ± 591.1	117 ± 14.1	187 ± 14.7	2.5 ± 0.6	640 ± 94.34

The data are shown as the mean ± standard deviation.

[a]Se(IV) was less than 20 μg/L.

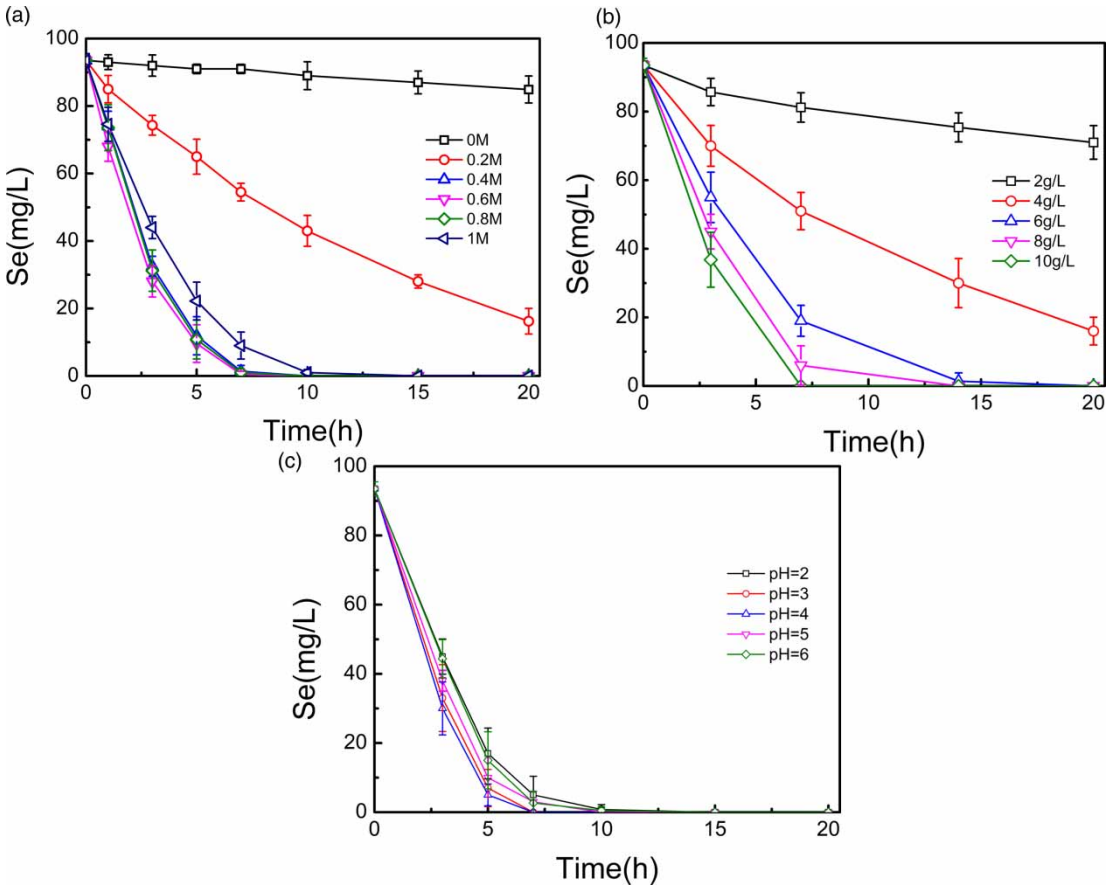

Figure 2 | Influence of (a) H_2O_2 concentration, (b) ZVI dosage and (c) initial pH values on Se(VI) removal. Initial Se(VI) concentration was 93.5 mg/L.

When the ZVI dosage was increased to 10 g/L, all the Se(VI) could be removed in 7 h. Thus, we set the optimal ZVI dosage to be 10 g/L to obtain rapid Se(VI) removal. In addition, Figure 2(c) shows that pH exerted little influence on Se(VI) removal. Thus, the P-ZVI-O method was capable to efficiently eliminate Se(VI) at acidic and neutral pH values.

Evolution of H_2O_2, Fe ions and zeta potential during ZVI pretreatment

To preliminarily probe the underlying mechanism for such exceptional properties of P-ZVI-O for Se(VI) removal, we first determined the variation of H_2O_2 concentration, Fe ions and zeta potential during the pretreatment process. As shown in Figure 3(a), 0.40 M of H_2O_2 were exhausted in 5 min, indicating that H_2O_2 was not involved in the subsequent Se(VI) removal. H_2O_2 reacts with ZVI strongly and produces magnetite (Fe_3O_4) under the conditions of this experiment, which can serve as a mediated layer for the Se(VI) enrichment and semiconductor for the electron transfer (Segura *et al.* 2015; Tang *et al.* 2016).

The Fe^{3+} concentration during acidic pretreatment remained at a low level due to the relative anaerobic condition caused by ZVI (Figure 3(b)). However, it is not the case for P-ZVI-O, and Fe^{3+} concentration increased sharply at the beginning of H_2O_2 pretreatment, while Fe^{2+} concentration increased very slowly in the first 5 min due to the presence of H_2O_2. After the complete consumption of H_2O_2 after 5 min (Figure 3(a)), Fe^{3+} concentration dropped sharply due to the gradual increase of pH, whereas Fe^{2+} concentration increased dramatically over the next 10 min, and finally reached 360 mg/L at 60 min. It is well known that ferrous (particularly Fe^{2+}) plays an important role in Se(VI) reduction indirectly and facilitating the transformation of the passive layer to magnetite via binding the iron surface. Therefore, the mass of Fe^{2+} can contribute to the effective removal of Se(VI) by P-ZVI-O.

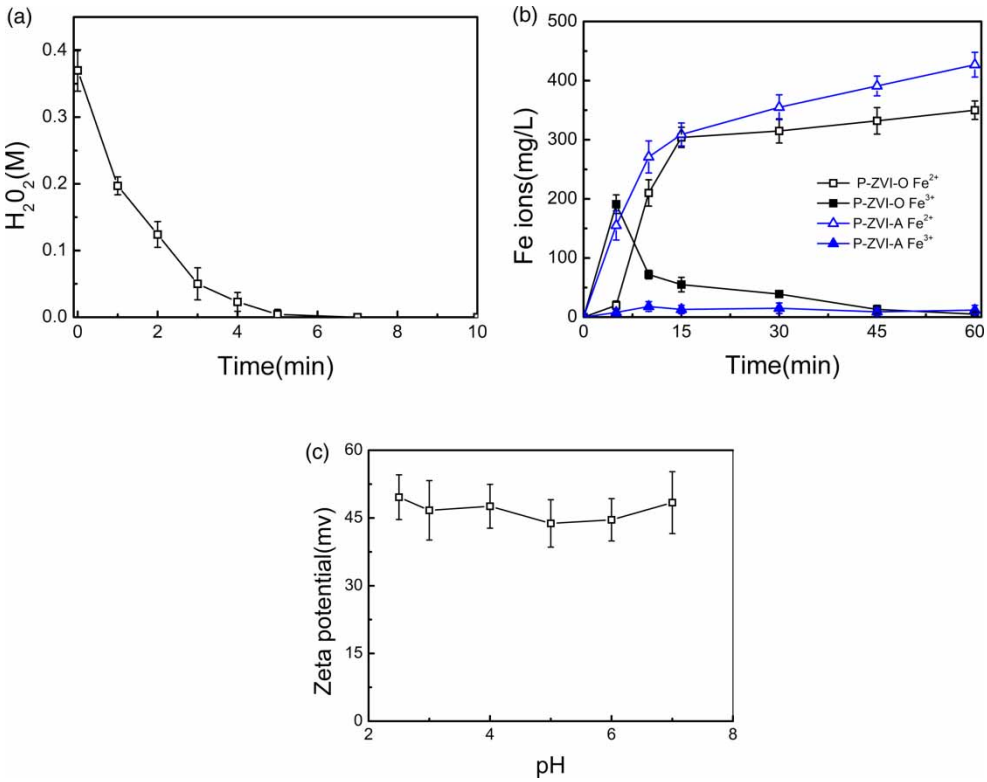

Figure 3 | Variation of (a) H_2O_2 concentration, (b) Fe ions concentration and (c) zeta potential during pretreatment process with the content of 10 g/L ZVI and 0.4 M H_2O_2.

Zeta potential reflects the electrostatic affinity of ferric substance toward Se(VI). The zeta potential values of the P-ZVI-O suspension were very high (>45 mV) in the pH range of 2.5–7 (Figure 3(c)). Note that they were not measured at pH ≥ 8 due to the precipitation of ferric substance. Such high zeta potential of P-ZVI-O indicated that ferric substances could exhibit a strong affinity toward SeO_4^{2-} anions. Furthermore, the charge repulsion is expected to promote the dispersion of tiny ferric substances in solution, which seems favorable to provide abundant reaction sites for the Se(VI) removal.

Evolution of pH and ORP values during Se removal

During Se(VI) removal by ZVI, ZVI-O, P-ZVI-A and P-ZVI-O, the variation of pH values as well as the oxidation–reduction potential (ORP) in wastewater were recorded. For all the four modes, pH values of the reaction systems increased at the beginning of the reactions (Figure 4(a)). However, the P-ZVI-A and P-ZVI-O modes could only result in the final pH increasing to ~5, while that of the ZVI-O mode could reach about 9. This is because simultaneous addition of ZVI and H_2O_2 exposed abundant inner matters to react with H^+ in solution (Segura *et al.* 2015).

ORP reflects the oxidation–reduction property of a given solution. Distinct ORP variations of the four modes were observed in Figure 4(b). The ZVI mode showed the highest positive potential during the whole reaction, possibly due to the hydrous ferric oxide covering the inner layer of ZVI and interdicting mass transport (Guan *et al.* 2015). The ORPs for the ZVI-O and P-ZVI-A modes varied around the zero line, which might result from SeO_4^{2-} and the reductive substances (Fe^0, Fe_3O_4, FeO and Fe^{2+}) (Tang *et al.* 2016; Makota *et al.* 2017). Comparatively, the ORP of P-ZVI-O mode declined rapidly to below −300 mV, showing a strong reducing potential of the P-ZVI-O reaction system. It is also well consistent with that of the Se(VI) removal. The ORP value reached the lowest point after 7-h reaction when Se(VI) was completely removed.

Evolution of the dissolved and surface-associated Fe^{2+} during Se removal

Considering the key role of the dissolved Fe^{2+} and surface-associated Fe^{2+} in the reductive process of ZVI/H_2O

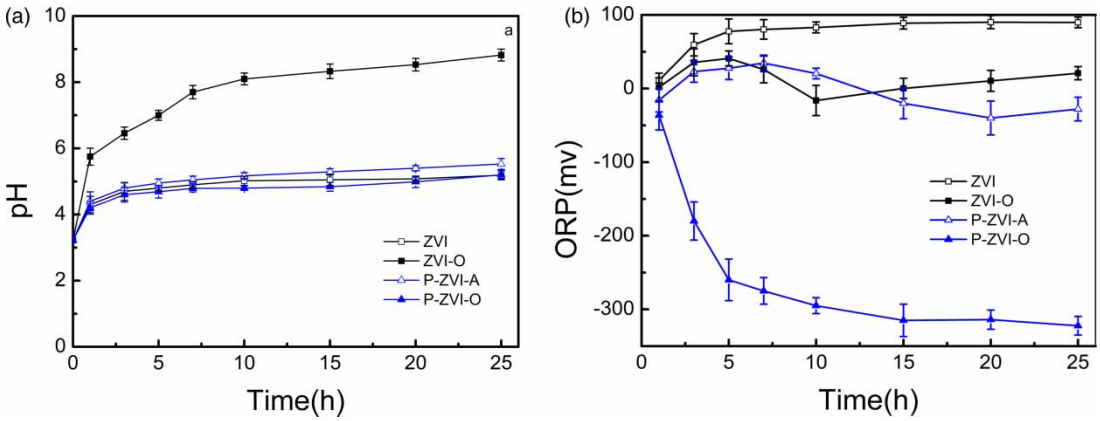

Figure 4 | Evolution of (a) pH and (b) ORP values during the reactions of four modes. Dosage of ZVI and H_2O_2 are 10 g/L and 0.4 M, respectively. Initial reaction pH is 3.2 ± 0.1.

system, their concentrations during Se(VI) removal were measured to better understand the reaction process. For the ZVI mode, the dissolved Fe^{2+} showed a slow drop from 60 mg/L to 50 mg/L within 25 h (Figure 5(a)), possibly because the consumption of contaminants and dissolved oxygen (Guan *et al.* 2015). Simultaneously, the surface-associated Fe^{2+} dropped sharply from >100 mg/L to <10 mg/L in 5 h (Figure 5(b)). For the ZVI-O mode, negligible dissolved Fe^{2+} was detected during the whole reaction, while the added H_2O_2 favored the initial generation of relative high concentration of the surface-associated Fe^{2+} via iron corrosion. With the consumption of the surface-associated Fe^{2+}, an obvious Se removal was observed in the first 7 h. As for P-ZVI-A, it caused the highest dissolved Fe^{2+} (>200 mg/L) at the beginning. However, it remained unchanged during the reaction, similar to the surface-associated Fe^{2+} of 16–20 mg/L. As a result, very low Se removal was realized, possibly due to the absence of corrosion products (e.g. Fe_3O_4) to provide active adsorption sites for Fe^{2+}. The P-ZVI-O mode resulted in an initial dissolved Fe^{2+} of >180 mg/L, which subsequently dropped sharply in the first 7 h and remained constant at ~100 mg/L finally. Furthermore, the adsorption of Fe^{2+} onto the iron oxides surface could release H^+, thereby maintained the pH values in the P-ZVI-O and P-ZVI-A mode. As for the ZVI-O mode, the weak buffering capacity due to the lack of Fe^{2+} in the presence of H_2O_2 resulted in a rapid rise of pH along with the corrosion of ZVI (Noubactep 2013). As one of high reactive iron species, the surface-associated Fe^{2+} decreased from 100 to ~60 mg/L. The variation was consistent with the removal curve of Se(VI), indicating that Fe^{2+} was involved in the Se(VI) reduction.

Characterization of ZVI before and after Se removal

Iron crystal and surface morphology were measured before and after Se removal reaction. For the P-ZVI-A mode, only the exposed Fe^0 was detected after acid pretreatment,

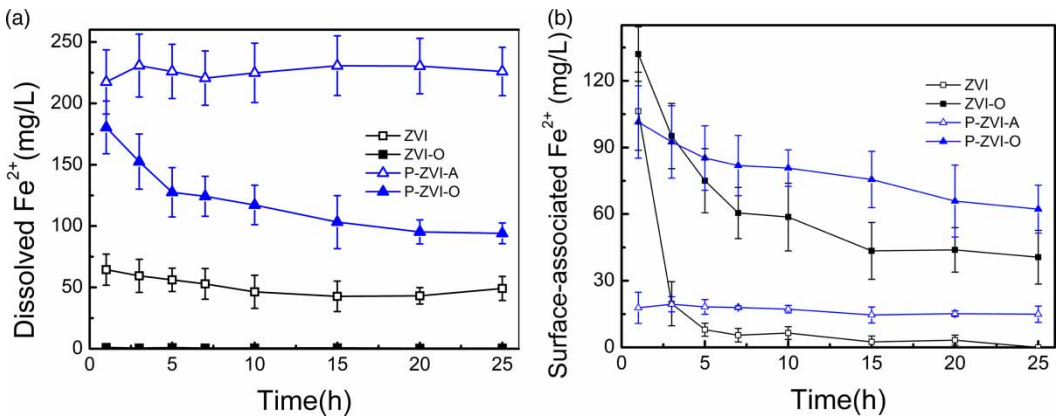

Figure 5 | Evolution of (a) dissolved Fe^{2+} and (b) surface-associated Fe^{2+} during Se removal. Dosage of ZVI and H_2O_2 were 10 g/L and 0.4 M, respectively. Initial reaction pH is 3.2 ± 0.1.

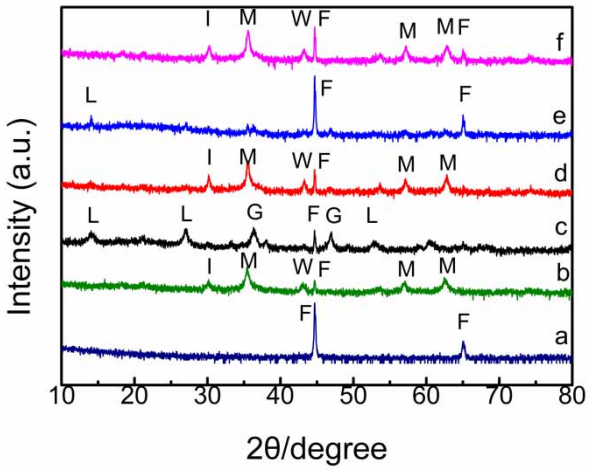

Figure 6 | XRD patterns of the solid samples for the four modes before and after Se removal. (a) fresh P-ZVI-A, (b) fresh P-ZVI-O, (c) ZVI after Se removal, (d) ZVI-O after Se removal, (e) P-ZVI-A after Se removal, (f) P-ZVI-O after Se removal. (F: Fe^0; M: magnetite; W: wüstite; I: iron oxide; L: lepidocrocite; G: goethite).

which was consistent with the pristine ZVI (Figure 6). As shown, the XRD data evidenced the presence of Fe_3O_4/FeO in the P-ZVI-O mode, suggesting the formation of Fe_3O_4 on the surface of ZVI as the major corrosion product during H_2O_2/HCl pretreatment. After reaction with the wastewater samples, the ZVI mode produced large amount of goethite and lepidocrocite to cover the inner Fe^0. Although hydrous ferric oxides possessed certain capacity for nonspecific Se(VI) and specific Se(IV) adsorption, they could not offer electron for Se(VI) reduction, and the electron transfer from the inner layer outside was interdicted by the lepidocrocite layer (Caré *et al.* 2013; Guan *et al.* 2015). For the ZVI-O mode after treatment, the presence of Fe^0 is available for electron donor and transfer for Se(VI) reduction. Also, Fe_3O_4/FeO acted as mediated surface for Se(VI) reduction (Tang *et al.* 2016). Fe^0 together with high concentration of Fe^{2+} for the P-ZVI-A mode exhibited rather poor removal of Se(VI) considering the weak affinity of Fe^0 toward Se(VI) for further reduction. Similar chemical composition of the P-ZVI-O mode was observed as the ZVI-O mode, where Fe^0 and Fe_3O_4/FeO could be distinguished in the XRD pattern. The difference between both modes was the corrosion strategy. The formation of Fe_3O_4/FeO for P-ZVI-O served as mediated interface to enhance the Se(VI) adsorption and subsequent reduction, along with promoting the electron transfer from inner Fe^0 core (Coelho *et al.* 2008; Tang *et al.* 2016).

As seen in Figure 7, the surface of pristine ZVI was smooth with a small quantity of cavities. Acid pretreatment destroyed the passive layer of ZVI but still kept the smooth surface. For the P-ZVI-O, abundant granular corrosion products formed on the surface after H_2O_2 pretreatment, that is, formation of magnetite (Fe_3O_4) layer. After reaction with Se(VI), the surface of pristine ZVI became irregular, with the corrosion products like rods and flaks, indicating the generation of goethite and lepidocrocite. Similarly, the surfaces of the ZVI-O and P-ZVI-A mode were intensively corroded, resulting in the formation of various corrosion products

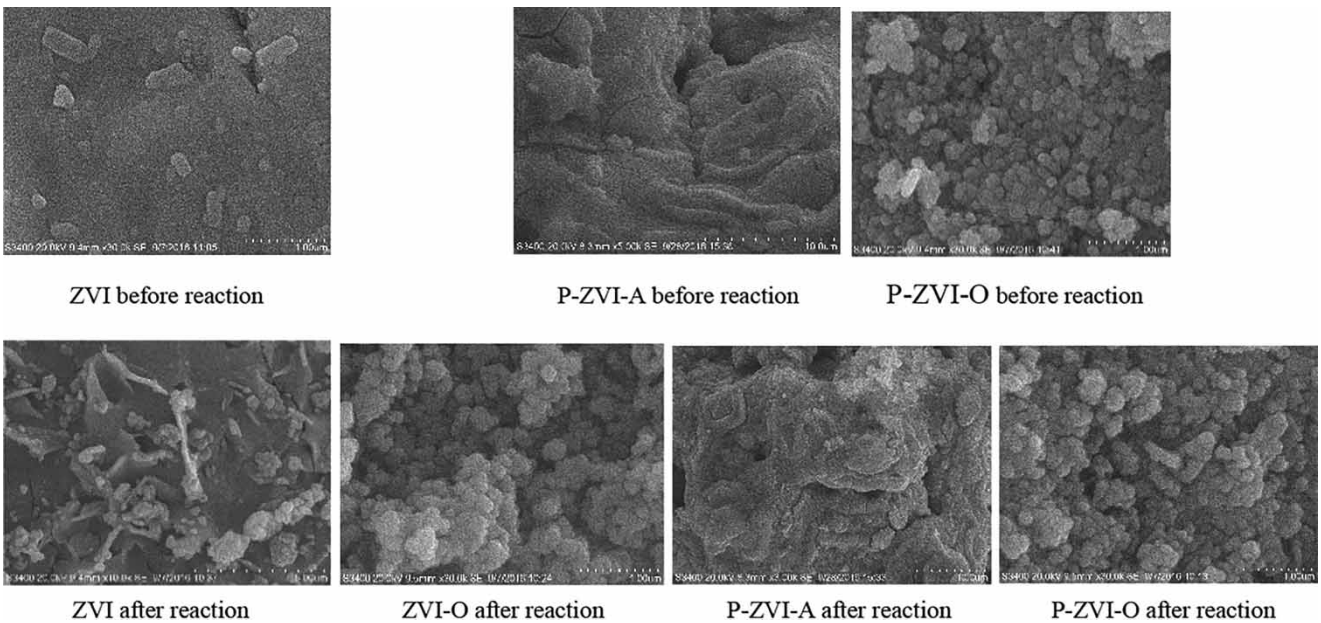

Figure 7 | Surface morphology of iron sludge after pretreatment and reaction with Se(VI).

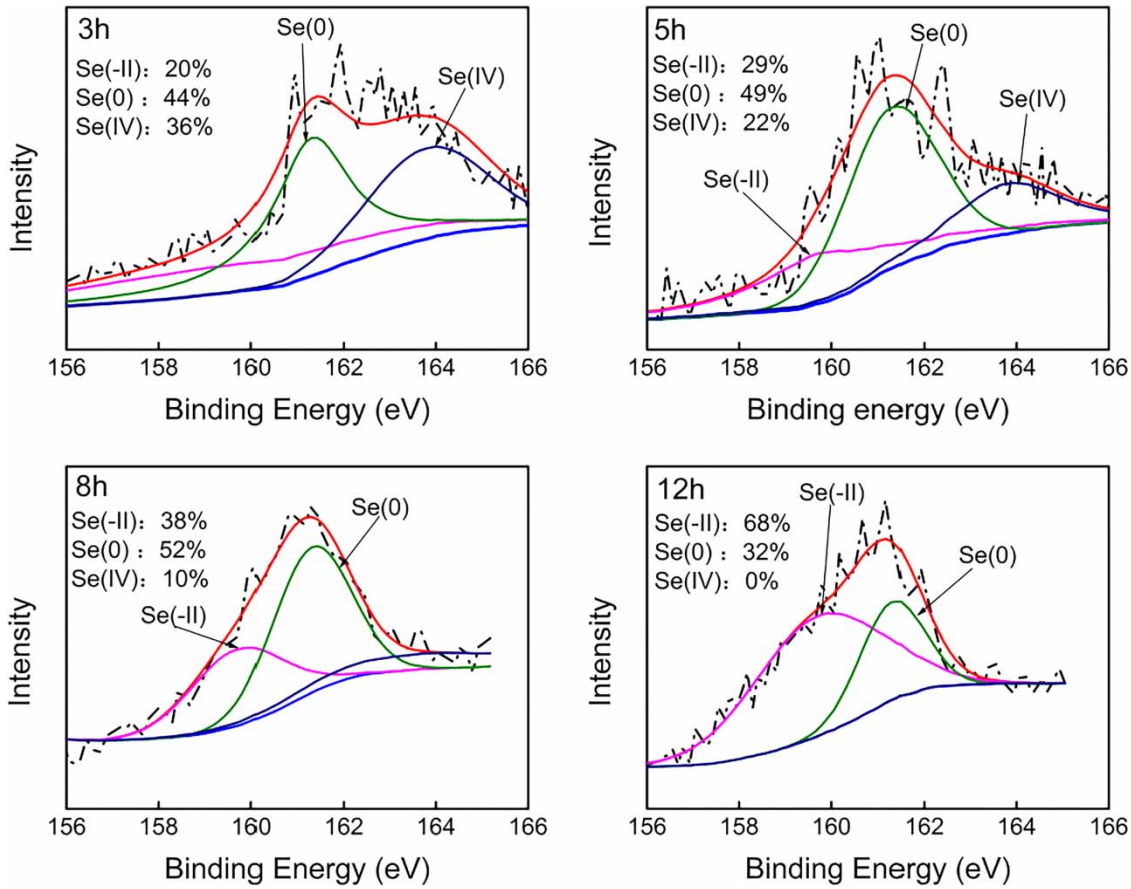

Figure 8 | Evolution of the Se valence in the solid phase of the P-ZVI-O mode.

containing magnetite and lepidocrocite. The iron oxides/hydroxides can eliminate Se(VI) via adsorption, and the magnetite favored its reductive transformation (Yang *et al.* 2016; Makota *et al.* 2017). However, the lepidocrocite played a passive role due to its electrical insulation (Mu *et al.* 2017).

Fate of Se after P-ZVI-O treatment

Evolution of the valence of Se sequestered on the solid phase of the P-ZVI-O is depicted in Figure 8. After 3-h reaction, Se(IV) was detected in the solid phase. The subsequent decrease of its concentration was observed due to the reductive transformation to Se(0) and Se(-II) according to the XPS results. It is consistent with the earlier results (Yang *et al.* 2016) that the increasing proportion of Se(0) and Se(-II) was observed over the reaction time for Se sequestered by iron based materials. Based on the above results, it could be inferred that Se(VI) was first captured by the solid surface via electrostatic attraction, then the adsorbed Se(VI) was subject to reduction to Se(IV), Se(0) and Se(-II) in sequence. Thus, the main pathways of Se(VI) reduction by P-ZVI-O are described as follows (Equations (1)–(6)) (Yoon *et al.* 2011; Klas & Kirk 2013):

$$Fe^0 \rightarrow Fe^{2+} + 2e^- \quad (1)$$

$$Fe(OH)_2 + OH^- \rightarrow Fe(OH)_3 + e^- \quad (2)$$

$$SeO_4^{2-} + 2H^+ + 2e^- \rightarrow SeO_3^{2-} + H_2O \quad (3)$$

$$SeO_3^{2-} + 6H^+ + 4e^- \rightarrow Se^0 + 3H_2O \quad (4)$$

$$2Fe^0 + HSeO_4^- + 2H^+ \rightarrow HSe^- + 2\gamma\text{-FeOOH} \quad (5)$$

$$2\gamma\text{-FeOOH} + Fe^{2+} \rightarrow Fe_3O_4 + 2H^+ \quad (6)$$

In summary, the enhanced Se(VI) reduction by P-ZVI-O indicated the favorable role of the H_2O_2/HCl pretreatment in the reductive performance of ZVI/H_2O system, where the constituent in the P-ZVI-O system, such as Fe^{2+}, surface-associated Fe^{2+}, Fe_3O_4 and ZVI, contributed to the enhanced removal of Se(VI). However, further study on the mechanism of positive role of H_2O_2/HCl pretreatment in Se(VI) removal by ZVI is still required and currently underway in our group.

CONCLUSIONS

In this study, we first demonstrated the enhanced Se(VI) reduction and removal from realistic mining effluent by ZVI pretreated with H_2O_2 under acidic pH, which was superior to other ZVI utilization modes, such as ZVI alone, pretreatment of ZVI with acid, and simultaneous addition of ZVI and H_2O_2 into realistic mining effluent. The H_2O_2/HCl pretreatment resulted in the generation of abundant reducing corrosion products (e.g. Fe_3O_4, FeO and Fe^{2+}), which could serve as reactive media to facilitate adsorption and reduction for Se(VI). Besides, the iron oxides could act as the mediated interface to provide adsorption sites and for Fe^{2+} ions bonding. The evolution of ZVI and Se during wastewater treatment suggested that the Se(VI) removal was realized via various pathways including adsorption, reduction and/or co-precipitation.

ACKNOWLEDGEMENTS

We appreciate the financial support from National Key Research and Development Program of China (grant No. 2016YFA0203104) and Natural Science Foundation of China (grant No. 51608255/51578280).

REFERENCES

Caré, S., Crane, R., Calabrò, P. S., Ghauch, A., Temgoua, E. & Noubactep, C. 2013 Modeling the permeability loss of metallic iron water filtration systems. *Clean-Soil, Air, Water* **41**, 275–282.

Coelho, F., Ardisson, J. D., Moura, F. C., Lago, R. M., Murad, E. & Fabris, J. D. 2008 Potential application of highly reactive Fe(0)/Fe_3O_4 composites for the reduction of Cr(VI) environmental contaminants. *Chemosphere* **71**, 90–96.

Fu, F. & Wang, Q. 2011 Removal of heavy metal ions from wastewaters: a review. *Journal of Environmental Management* **92**, 407–418.

Guan, X., Sun, Y., Qin, H., Li, J., Lo, I. M., He, D. & Dong, H. 2015 The limitations of applying zero-valent iron technology in contaminants sequestration and the corresponding countermeasures: the development in zero-valent iron technology in the last two decades (1994–2014). *Water Research* **75**, 224–248.

Guo, X., Yang, Z., Dong, H., Guan, X., Ren, Q., Lv, X. & Jin, X. 2016 Simple combination of oxidants with zero-valent-iron (ZVI) achieved very rapid and highly efficient removal of heavy metals from water. *Water Research* **88**, 671–680.

Kang, S. Y., Lee, J. U., Moon, S. H. & Kim, K. W. 2004 Competitive adsorption characteristics of Co^{2+}, Ni^{2+}, and Cr^{3+} by IRN-77 cation exchange resin in synthesized wastewater. *Chemosphere* **56**, 141–147.

Kang, M., Ma, B., Bardelli, F., Chen, F., Liu, C., Zheng, Z., Wu, S. & Charlet, L. 2013 Interaction of aqueous Se(IV)/Se(VI) with FeSe/$FeSe_2$: implication to Se redox process. *Journal of Hazardous Materials* **248–249**, 20–28.

Katsoyiannis, I. A., Voegelin, A., Zouboulis, A. I. & Hug, S. J. 2015 Enhanced As(III) oxidation and removal by combined use of zero valent iron and hydrogen peroxide in aerated waters at neutral pH values. *Journal of Hazardous Materials* **297**, 1–7.

Klas, S. & Kirk, D. W. 2013 Understanding the positive effects of low pH and limited aeration on selenate removal from water by elemental iron. *Separation and Purification Technology.* **116**, 222–229.

Liang, L., Sun, W., Guan, X., Huang, Y., Choi, W., Bao, H., Li, L. & Jiang, Z. 2014 Weak magnetic field significantly enhances selenite removal kinetics by zero valent iron. *Water Research* **49**, 371–380.

Ling, L., Pan, B. & Zhang, W. X. 2015 Removal of selenium from water with nanoscale zero-valent iron: mechanisms of intraparticle reduction of Se(IV). *Water Research* **71**, 274–281.

Makota, S., Nde-Tchoupe, A. I., Mwakabona, H. T., Tepong-Tsindé, R., Noubactep, C., Nassi, A. & Njau, K. N. 2017 Metallic iron for water treatment: leaving the valley of confusion. *Applied Water Science* **7**, 1–20.

Mu, Y., Jia, F., Ai, Z. & Zhang, L. 2017 Iron oxide shell mediated environmental remediation properties of nano zero-valent iron. *Environmental Science: Nano* **4**, 27–45.

Nancharaiah, Y. V. & Lens, P. N. L. 2015 Selenium biomineralization for biotechnological applications. *Trends in Biotechnology* **33**, 323–330.

Noubactep, C. 2013 Relevant reducing agents in remediation Fe^0/H_2O systems. *Clean – Soil Air Water* **41**, 493–502.

Segura, Y., Martínez, F., Melero, J. A. & Fierro, J. L. G. 2015 Zero valent iron (ZVI) mediated Fenton degradation of industrial wastewater: treatment performance and characterization of final composites. *Chemical Engineering Journal* **269**, 298–305.

Tang, C., Huang, Y. H., Zeng, H. & Zhang, Z. 2014 Reductive removal of selenate by zero-valent iron: the roles of aqueous Fe^{2+} and corrosion products, and selenate removal mechanisms. *Water Research* **67**, 166–174.

Tang, C., Huang, Y., Zhang, Z., Chen, J., Zeng, H. & Huang, Y. H. 2016 Rapid removal of selenate in a zero-valent iron/Fe_3O_4/Fe^{2+} synergetic system. *Applied Catalysis B: Environmental* **184**, 320–327.

Winkel, L. H., Johnson, C. A., Lenz, M., Grundl, T., Leupin, O. X., Amini, M. & Charlet, L. 2012 Environmental selenium research: from microscopic processes to global understanding. *Environmental Science & Technology* **46**, 571–579.

Xie, W., Liang, Q., Qian, T. & Zhao, D. 2015 Immobilization of selenite in soil and groundwater using stabilized Fe-Mn binary oxide nanoparticles. *Water Research* **70**, 485–494.

Yang, Z., Shan, C., Zhang, W., Jiang, Z., Guan, X. & Pan, B. 2016 Temporospatial evolution and removal mechanisms of As(V) and Se(VI) in ZVI column with H_2O_2 as corrosion accelerator. *Water Research* **106**, 461–469.

Yang, Z., Ma, X., Shan, C., Fang, Z. & Pan, B. 2018a Enhanced nitrobenzene reduction by zero valent iron pretreated with H_2O_2/HCl. *Chemosphere* **197**, 494–501.

Yang, Z., Shan, C., Mei, Y., Jiang, Z., Guan, X. & Pan, B. 2018b Improving reductive performance of zero valent iron by H_2O_2/HCl pretreatment: a case study on nitrate reduction. *Chemical Engineering Journal* **334**, 2255–2263.

Yoon, I. H., Kim, K. W., Bang, S. & Kim, M. G. 2011 Reduction and adsorption mechanisms of selenate by zero-valent iron and related iron corrosion. *Applied Catalysis B: Environmental* **104**, 185–192.

Yoon, I. H., Yoo, G., Hong, H. J., Kim, J., Kim, M. G., Choi, W. K. & Yang, J. W. 2016 Kinetic study for phenol degradation by ZVI-assisted Fenton reaction and related iron corrosion investigated by X-ray absorption spectroscopy. *Chemosphere* **145**, 409–415.

First received 27 September 2018; accepted in revised form 18 December 2018. Available online 28 December 2018